

# Berezinskii–Kosterlitz–Thouless transition on regular and Villain types of $q$ -state clock models

Tasrief Surungan<sup>1</sup>, Shunsuke Masuda<sup>2</sup>, Yukihiro Komura<sup>2,3</sup> and Yutaka Okabe<sup>2</sup>

<sup>1</sup> Department of Physics, Hasanuddin University, Makassar, South Sulawesi 90245, Indonesia

<sup>2</sup> Department of Physics, Tokyo Metropolitan University, Hachioji, Tokyo 192-0397, Japan

<sup>3</sup> CIJ-solutions, Chuo-ku, Tokyo, 103-0023, Japan

E-mail: [tasrief@unhas.ac.id](mailto:tasrief@unhas.ac.id) and [okabe@phys.se.tmu.ac.jp](mailto:okabe@phys.se.tmu.ac.jp)

Received 27 September 2018, revised 14 April 2019

Accepted for publication 17 May 2019

Published 5 June 2019



CrossMark

## Abstract

We study  $q$ -state clock models of regular and Villain types with  $q = 5, 6$  using cluster-spin updates and observed double transitions in each model. We calculate the correlation ratio and size-dependent correlation length as quantities for characterizing the existence of Berezinskii–Kosterlitz–Thouless (BKT) phase and its transitions by large-scale Monte Carlo simulations. We discuss the advantage of correlation ratio in comparison to other commonly used quantities in probing BKT transition. Using finite size scaling of BKT type transition, we estimate transition temperatures and corresponding exponents  $\eta$ . The comparison between the results from both types revealed that the existing transitions belong to BKT universality.

Keywords: clock model, Villain model, Kosterlitz–Thouless transition, Monte Carlo simulation, cluster spin update

(Some figures may appear in colour only in the online journal)



Original content from this work may be used under the terms of the [Creative Commons Attribution 3.0 licence](https://creativecommons.org/licenses/by/3.0/). Any further distribution of this work must maintain attribution to the author(s) and the title of the work, journal citation and DOI.

## 1. Introduction

The two-dimensional (2D)  $q$ -state clock models play an important role in the study of phase transitions as they provide links between several seminal works [1–5]. The underlining  $Z_q$  symmetry is a generalization of  $Z_2$  Ising model, the most studied and the first model in statistical physics found to exhibit a phase transition [1]. The XY model, their continuous counterpart, is the native host of a unique phase which is the only type of order allowed by the well known Mermin–Wagner theorem [2] for a 2D pure system with continuous symmetry. It is a quasi-long-range order (QLRO) called Berezinskii–Kosterlitz–Thouless (BKT) phase [3–5]; essentially a state with bound vortex–antivortex pairs. The BKT phase is ubiquitous for many systems, observed for example in a planar array of coupled Josephson junctions in transverse magnetic field [6, 7], liquid crystal [8] and the low-dimensional ferroelectrics [9]. Interestingly, this type of phase is inherited by the clock models, depending on the parameter  $q$  which evenly divides  $2\pi$  into  $q$  equal angles.

Based on the Mermin–Wagner theorem above mentioned, a discrete symmetry is important for the existence of a true LRO in 2D systems. It was theoretically predicted [10, 11] and later confirmed numerically by several early studies [12–14] that the  $q$ -state clock models experience two transitions for  $q > 4$ , i.e. the lower ( $T_1$ ) and the higher temperature ( $T_2$ ) transitions, where the BKT phase exists between them, which is characterized by of vortex–antivortex pairs becoming bound. Mathematically, this allows the phase to be characterized by the power-law behavior of the spin–spin correlation function. Since it is not possible to obtain such a formation out of spins with  $Z_q$  symmetry for  $q \leq 4$ , the corresponding models cannot host a BKT phase. A relatively small excitation is not allowed as any possible change of angular directions is always large. This leads the low-temperature excitation to be occupied by a true LRO, rather than BKT phase. For  $q > 4$  there is an interplay between the discreteness which tends to create an LRO at low temperature and the inherited symmetry trying to preserve BKT phase. The conformity of both causes the LRO to exist below the BKT phase. Thereby two transition temperatures,  $T_1 < T_2$ , are observed; each corresponds to transition between LRO and QLRO and between QLRO and a disordered phase. The LRO is induced by the discrete symmetry of the clock model.

In recent years, the study of phase transition of  $q$ -state clock models has regained a lot of interest, in particular to probe whether the existing double transitions are BKT-type or not [15–21]. Analytical results from a related model called Villain model [22] revealed that both transitions are BKT type and interconnected via duality relation [11] for  $q > 4$ . Although such relation does not exist in the regular clock models, the renormalization group study [10] as well as standard Monte Carlo studies [12, 23] pointed out two separate transitions belonging to BKT universality. This is in contrast to the report by Lapilli *et al* [15] who suggested that the transitions are BKT type only for  $q \geq 8$ . A study based on Fisher zero approach claimed that the transitions for  $q = 6$  are not BKT type [16], which could possibly be an artifact result from small system sizes [17]. While observing double transitions for  $q = 5, 6$ , Baek *et al* [18, 19] concluded that transitions are BKT type for  $q = 6$ , but not for  $q = 5$  due to the role played by the supposed residual symmetry  $Z_5$ . However, more recent studies by Kumano *et al* [20] and by Chatelain [21] are in favor of the previous scenario that the two transitions belonging to BKT type. With these conflicting results, the controversy on the type of phase transitions of  $q$ -state clock models is mainly related to  $q = 5, 6$ . Further investigation using different approaches is required, primarily to study  $q$ -state clock models for  $q = 5, 6$ .

In this paper, we report our study on these particular models, and try to address the controversy. We perform numerical studies on regular (cosine) and Villain types of the models. The Villain type is quite interesting due to the existence of exact duality transformation by which

the lower and higher temperature transitions are interconnected. Due to the similarity of the underlining symmetry with the clock models, studying Villain model can bring a clear insight related to the debated issue; in particular if one uses the correlation ratio in characterizing the BKT transition. We argue that this quantity is more straightforward and exceptionally suitable in capturing the double transitions.

The remaining part of the paper is organized as follows: section 2 describes the models and the method. The results are discussed in section 3 while section 4 is devoted to the concluding remarks. Supplementary subjects are discussed in appendices.

## 2. Models and simulation method

A  $q$ -state clock model of regular (cosine) type is defined by the following Hamiltonian

$$H = -J \sum_{\langle ij \rangle} \vec{s}_i \cdot \vec{s}_j = -J \sum_{\langle ij \rangle} \cos(\theta_i - \theta_j), \quad (1)$$

where spins  $\vec{s}_i$  on lattice sites are planar spins restricted to align in  $q$  discrete angles ( $\theta = 2n\pi/q$  with  $n = 1, \dots, q$ ). The sum is over nearest-neighbor sites of square lattice ( $L \times L$ ), with periodic boundary conditions. The interaction is ferromagnetic ( $J > 0$ ) by which all spins are aligned in the ground state configuration with  $q$ -fold degeneracy; the ground state energy is  $E_{\text{gs}} = -2NJ$  for the square lattice.

By rewriting equation (1) as  $H = -J \sum_{\langle ij \rangle} V(\theta_{ij})$  with  $\theta_{ij} = \theta_i - \theta_j$ , we can assign a local Boltzmann factor for the clock model as  $\exp[\kappa V(\theta_{ij})] = \exp[\kappa \cos(\theta_{ij})]$ , where  $\kappa = \beta J$  with  $\beta$  as the inverse temperature. Villain type of clock model is obtained by introducing a set of auxiliary fields [11, 22]. For the Villain model, the local Boltzmann factor is given by

$$\exp[\kappa V_{\text{Vil}}(\theta_{ij})] = \sum_{m=-\infty}^{\infty} \exp\left[-\frac{\kappa}{2}(\theta_{ij} - 2\pi m)^2\right]. \quad (2)$$

The result of the summation of Gaussian function in equation (2) over  $m$  yields a similar form to the local Boltzmann factor of the clock model. The energy origin had better be shifted as  $\cos(\theta_{ij}) - 1$  for comparison. As we consider the regular (cosine) and Villain types of the models for  $q = 5, 6$ , there are four models altogether.

For a reliable calculation, we use the canonical Monte Carlo method with cluster spin updates proposed by Swendsen and Wang [24] and adopt the embedded scheme of Wolff [25] in constructing a cluster for clock spins. A cluster spin algorithm is crucial for Monte Carlo study in order to avoid drawback of single spin update which is frequently suffering from slowing down near the critical point. This is done by projecting the spins into a randomly selected orientation, out of  $q$  possibilities, so that the spins are divided into two groups (Ising-like spins). The embedded scheme is essential in carrying out cluster algorithm for such multi-component spins as planar and Heisenberg spins. After the projection, the original step of the cluster algorithm is performed, i.e. by connecting the spin to its nearest neighbors of the same group, with suitable probability depending on the local Boltzmann factor [26]. Spins in the cluster are updated at a time. One Monte Carlo step (MCS) is defined as updating all the spins.

We make measurement for the systems of linear size up to  $L = 512$ . In the careful discussion on the helicity modulus, which will be given in appendix A, we treat large enough sizes up to  $L = 2048$ . For the calculation of large systems, we use the GPU-based algorithm for the Swendsen–Wang algorithm [27], which is efficient for high-performance computing. Measurement is performed after enough equilibration steps ( $2 \times 10^4$  MCS's). Each data point is obtained from the average over several parallel runs, with  $4 \times 10^5$  MCS's for each run.

Typically, 5 measurements are done for each system size in order to estimate statistical errors. This means, each data point is obtained from the average of  $2 \times 10^6$  samples.

### 3. Results

#### 3.1. BKT transitions and correlation ratio

A BKT phase is essentially a state with bound vortex–antivortex pairs [4, 5]. In the case of XY model, the unbinding of these pairs at high temperature is assigned as BKT transition which separates the BKT phase and paramagnetic phase. It corresponds to the  $T_2$  transition of the clock models which have additional lower-temperature ( $T_1$ ) transition. The disappearance of bound vortex–antivortex pairs following the unbinding scenario at high temperatures is associated with the vanishing of helicity modulus  $\Upsilon$  [28, 29]. We briefly discuss this quantity in appendix A and present the result for examining the existing BKT phase of the 5-state and the 6-state clock model. Although this quantity is commonly used to probe BKT transition, it is not quite precise in characterizing the  $T_1$  transition as the disappearance of vortex–antivortex pairs at low temperature follows different mechanism. In the case of the clock model, the spin-wave excitations are prohibited due to the energy gap of discrete models at low temperatures. Thus, the origin of the disappearance of the bound vortex–antivortex pairs with the  $T_1$  transition is due to the discrete symmetry of the clock models. The conflicting main conclusions reported by [18, 19] and [21] suggest a more accurate way of calculating the helicity modulus when dealing with BKT transitions of the clock models [20].

A quantity called correlation ratio [30] is particularly applicable to probing BKT transitions both for the upper and the lower transitions, and has been used in various cases [31–33]. It is a ratio of correlation functions with different distances. At a critical point or line (BKT phase), the correlation function  $g(r)$  for an infinite system decays as a power of distance  $r$ ,

$$g(r) = \left\langle \frac{1}{L^D} \sum_i \vec{s}_i \cdot \vec{s}_{i+r} \right\rangle \sim r^{-(D-2+\eta)}, \quad (3)$$

where  $D$  and  $\eta$  are respectively the lattice dimension and decay exponent. The angular bracket denotes the thermal average. It incorporates two length ratios for a finite system of linear system size  $L$  away from the critical point or line,

$$g(r) \sim r^{-(D-2+\eta)} h(r/L, L/\xi) \quad (4)$$

with a correlation length  $\xi$  for the infinite system. The ratio of correlation functions of different distances,

$$\frac{g(r)}{g(r')} = \left( \frac{r}{r'} \right)^{-(D-2+\eta)} \frac{h(r/L, L/\xi)}{h(r'/L, L/\xi)} \quad (5)$$

will have a single scaling variable for finite size scaling (FSS),

$$\frac{g(r)}{g(r')} = \tilde{f}(L/\xi) \quad (6)$$

if we fix two ratios  $r/r'$  and  $r/L$ . In principle, one can take any pair of distances, but for the convenience of numerical calculation we choose  $r = L/2$  and  $r' = L/4$ .

At the critical region, where the correlation length  $\xi$  is infinite, the correlation ratio, equation (6), does not depend on the system size  $L$ . Thus, it is natural to expect a presence of a

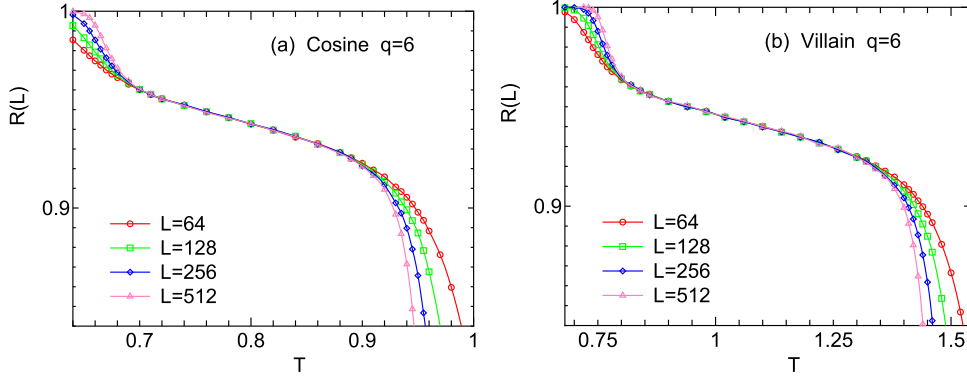


**Figure 1.** Temperature dependence correlation ratio,  $R(L) = g(L/2)/g(L/4)$ , for (a) regular and (b) Villain types for  $q = 6$ . The BKT phase and transitions are respectively indicated by the collapsed lines in the intermediate temperature and points where lines start separating. The error bar, in average, is in the order of symbol size.

crossing point for the existence of a continuous transition or collapsing curves for that of BKT phase in the plot of temperature dependence of correlation ratio for different system sizes.

We plot, as shown in figure 1, the temperature dependence of the correlation ratio,

$$R(L) = g(L/2)/g(L/4), \quad (7)$$

for  $q = 6$  of (a) regular and (b) Villain types, respectively. The plots have three typical temperature regimes, i.e. the lower, the intermediate and the upper regime. Each is associated with LRO, the BKT phase and the paramagnetic phase. The BKT phase is indicated by the collapsing curves of different system sizes. It is a direct consequence of power law behavior of correlation function at BKT phase. The spray out of the curves at lower and higher temperatures signifies two separated transitions.

The overall behavior of the correlation ratio, depicted in figure 1, is essentially the same for the model of regular type and that of Villain type. For the Villain model, the upper and the lower transitions are interconnected via an exact duality relation [11],

$$T_1 T_2 = \frac{4\pi^2}{q^2}. \quad (8)$$

In deriving equation (8), it is helpful to show the exact duality transformation of the partition function for the Villian model [11, 34];

$$\begin{aligned} Z &= \sum_{\xi} \prod_{\langle ij \rangle} \sum_{m=-\infty}^{\infty} e^{-\frac{K}{2} \left( \frac{2\pi}{q} (\xi_i - \xi_j) - 2\pi m \right)^2} \\ &= q^{-1-N} \sum_{\mu} \prod_{\langle ij \rangle} \frac{q}{\sqrt{2\pi K}} \sum_{m=-\infty}^{\infty} e^{-\frac{q^2}{8\pi^2 K} \left( \frac{2\pi}{q} (\mu_i - \mu_j) - 2\pi m \right)^2}. \end{aligned} \quad (9)$$

Here,  $\xi_i$  takes a value of  $1, \dots, q$  and  $\mu_i$ , a variable on a dual lattice, also takes a value of  $1, \dots, q$ . In the right-hand side, the summation is taken over the nearest-neighbor pairs in the dual lattice. Since the inverse temperature for the dual lattice,  $K^*$ , is regarded as

$$\frac{K^*}{2} = \frac{q^2}{8\pi^2 K},$$

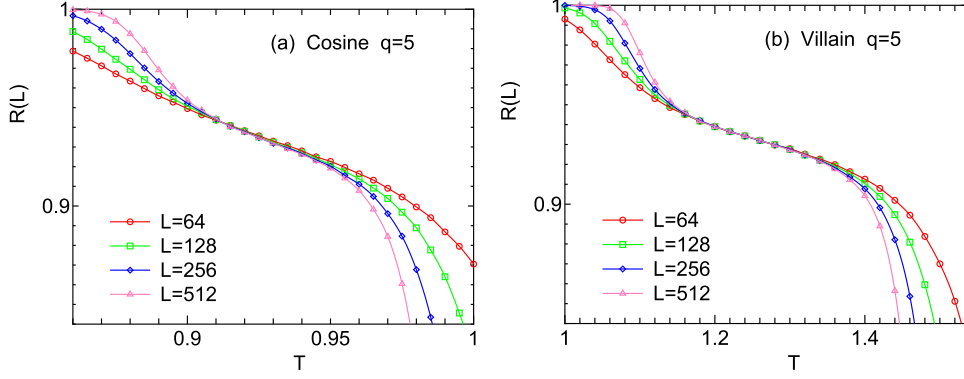


**Figure 2.** Temperature dependence of correlation ratio for different system sizes of (a) regular and (b) Villain types for  $q = 5$ . The typical pattern for the existence of BKT phase preserves except that the temperature range at which curves are collapsing becomes narrow.

we can easily obtain the duality relations between the two transitions, equation (8). Although there is not an exact duality relation for the regular clock model, quantitative data shown in figure 1 strongly suggest the universality of two transitions for regular and Villain types of  $q = 6$  clock model.

Analogous to figure 1, we plot the correlation ratio of (a) regular and (b) Villain types for  $q = 5$  in figure 2. The typical pattern of correlation ratio indicating the existence of BKT phase preserves, except that the collapsing regime becomes narrow, which indicates that the two transitions are getting closer. The discreteness suppresses the lower temperature excitation, but it does not totally rule out the BKT phase. Since the pattern of regular type is similar to that of Villain model, we argue that the transitions of 5-state clock model are also BKT type. The precise estimates of transition temperatures and the corresponding exponents are presented in the next sub-section.

The excellent performance of correlation ratio in characterizing the existence of BKT transition is related to the fact that it directly incorporates the correlation function, whose algebraic decay at BKT phase is a typical characteristic. We note that although the Binder ratio [35], essentially the moment ratio, has the same FSS property as in equation (6), the behavior of the collapsing and spraying out is not good due to the large corrections to FSS [30, 36].

We also calculate the size-dependent 2nd-moment correlation length for finite system,  $\xi(L)$ , which is defined as

$$\xi(L) = \frac{[\chi(0)/\chi(2\pi/L) - 1]^{1/2}}{2 \sin(\pi/L)} \quad (10)$$

with

$$\chi(k) = \frac{1}{N} \left| \left\langle \sum_r s(r) e^{ikr} \right\rangle \right|^2. \quad (11)$$

The quantity  $\xi(L)/L$  has a FSS property similar to equation (6), and has been frequently used in spin glass problems [37]. In this case again, the FSS of the Binder ratio [35] is not good compared to that of  $\xi(L)/L$ .

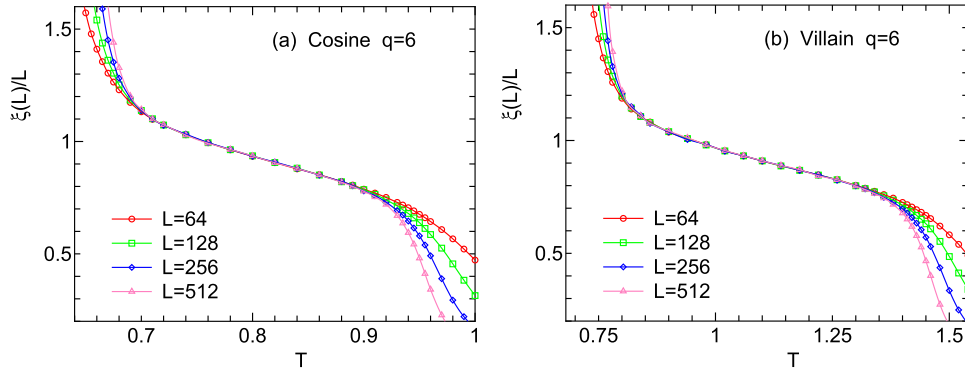


**Figure 3.** Temperature dependence of  $\xi(L)/L$  for different system sizes of (a) regular and (b) Villain types for  $q = 6$ . The typical pattern for the existence of BKT phase preserves.

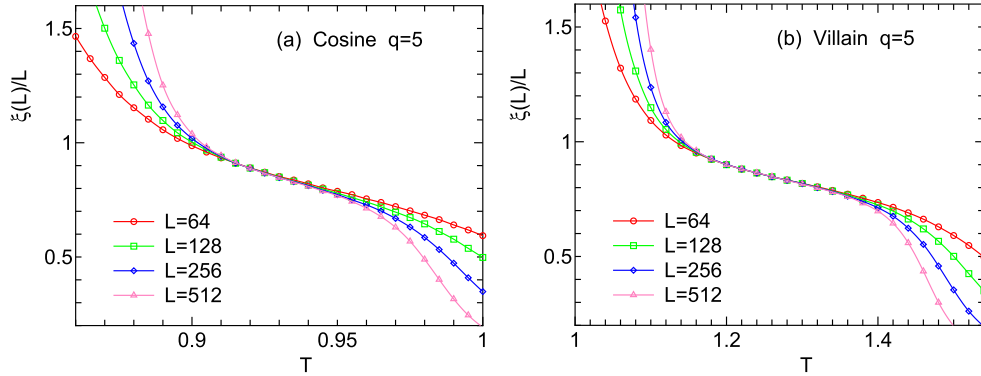


**Figure 4.** Temperature dependence of  $\xi(L)/L$  for different system sizes of (a) regular and (b) Villain types for  $q = 5$ . The typical pattern for the existence of BKT phase preserves except that the temperature range at which curves are collapsing becomes narrow.

We plot  $\xi(L)/L$  for the regular and Villain types of  $q = 6$  in figure 3. The collapsing curves at intermediate temperature regime and the spray out at lower and higher temperatures were observed at both types of models. This is another indication that the transitions of Villain and the regular types are of the same universality. For  $q = 5$ , shown in figure 4, the temperature range in which curves are collapsing becomes narrow; it is consistent with what observed for the correlation ratio shown in figure 2. All the data and plots presented thus far indicate that the transitions of  $q$ -state clock models of both types for  $q = 5, 6$  are universal.

### 3.2. FSS and the estimate of critical parameters

FSS is a standard technique in the study of phase transition. It is used to extract critical parameters from the finite system sizes. Here, we present FSS analysis based on diverging behavior of correlation length at BKT phase,

$$\xi \propto \exp(c/\sqrt{t}) \tag{12}$$

with  $t = (T - T_{\text{BKT}})/T_{\text{BKT}}$ . We choose  $T_{\text{BKT}}$  and a constant  $c$  such that all the data points are collapsed on a single curve.

The FSS plot of the correlation ratio, whose original data is given in figure 1, is shown in figure 5, associated with the data for  $q = 6$  of regular and Villain models. The plot is obtained by rescaling the horizontal axis,  $L/\xi$ . The scaled variable  $X(c, t)$  is defined by

$$X(c, t) = \frac{L}{\exp(c/\sqrt{t})} = \frac{L}{\exp(c/\sqrt{|(T - T_{\text{BKT}})/T_{\text{BKT}}|})}; \quad (13)$$

$c$  and  $T_{\text{BKT}}$  fitting parameters, are  $c_1$  and  $T_1$  for lower-temperature transition, and they are  $c_2$  and  $T_2$  for higher-temperature transition. Choosing several pairs of  $c_1$  and  $T_1$  as well as  $c_2$  and  $T_2$ , we obtained the fits for the estimated values. Our estimate for  $T_1$  and  $T_2$  for the regular model are respectively 0.701(5) and 0.898(5); while for the Villain model  $T_1 = 0.826(5)$  and  $T_2 = 1.326(5)$ . The numbers in parentheses are the uncertainty for the last digits. The transition temperatures for the Villain model are higher.

Similar procedure is applied to obtain plot shown in figure 6, which is the FSS plot of figure 2, associated with the data for regular and Villain models for  $q = 5$ . The estimates of  $T_1$  and  $T_2$  transition temperatures for regular model are respectively 0.911(5) and 0.940(5). The two transitions are very close to each other in comparison to the transitions for  $q = 6$  of the same model. This is related to the role played by the discreteness which almost rules out the BKT phase. For the Villain model, the estimate for  $T_1$  and  $T_2$  are respectively 1.182(5) and 1.335(5). Here, the temperature range is relatively wider compared to that of regular case.

The obtained set of transition temperatures,  $T_1$ 's and  $T_2$ 's, are tabulated in table 1, where the duality relation (equation (8)) are checked for the Villain type. As indicated, the duality relation is verified, both for  $q = 6$  and  $q = 5$ , which indicates the accuracy of the present calculation.

### 3.3. FSS without estimating $T_{\text{BKT}}$

We here perform the FSS analysis without estimating  $T_{\text{BKT}}$  to investigate the universality of the BKT transition. Such approach was recently employed in the study of the generalized XY model [38], where the analysis for the Potts model [39, 40] was applied to the study of the BKT transition. We focus on the FSS property of the ratio of the correlation ratio of different sizes, that is,  $R(2L)/R(L)$ .

We plot  $R(2L)/R(L)$  as a function of  $R(L)$  in figure 7 for four models, (a) regular and (b) Villain models for  $q = 6$  and (c) regular and (d) Villain models for  $q = 5$ . The lattice size pairs  $L - 2L$  with  $L = 64, 128$  and  $256$  are used. All the data for different sizes are collapsed on a single curve for each model. That is, the FSS is very good, although logarithmic corrections might not be small in the BKT transition [5, 41]. The value of  $R(2L)/R(L)$  remains 1 for the intermediate BKT phase, and becomes smaller than 1 for smaller  $R(L)$ , which means  $T > T_2$ , as in the XY model [38]. The regime at which the collapsing curves are parallel to the horizontal axis with the value of 1 is equivalent to the collapsing regime of the plot in figures 1 and 2, the regime for the existence of BKT phase. For clock model of  $q = 5, 6$ , the value of  $R(2L)/R(L)$  becomes larger than 1 for larger  $R(L)$ , that is,  $T < T_1$ , and comes back to 1 for  $R(L) = 1$ , that is,  $T = 0$ ; this behavior comes from the ordered phase.

We assign the values of  $R(L)$  at  $T_1$  and  $T_2$  as  $R_1$  and  $R_2$ , respectively. The values of  $R_1$  and  $R_2$  of regular model and Villain model are very close but there is a small difference for  $q = 6$ . For  $q = 5$ , the intermediate region becomes narrower, and the difference of regular and Villain models becomes more appreciable. The overall FSS behaviors of regular and Villain

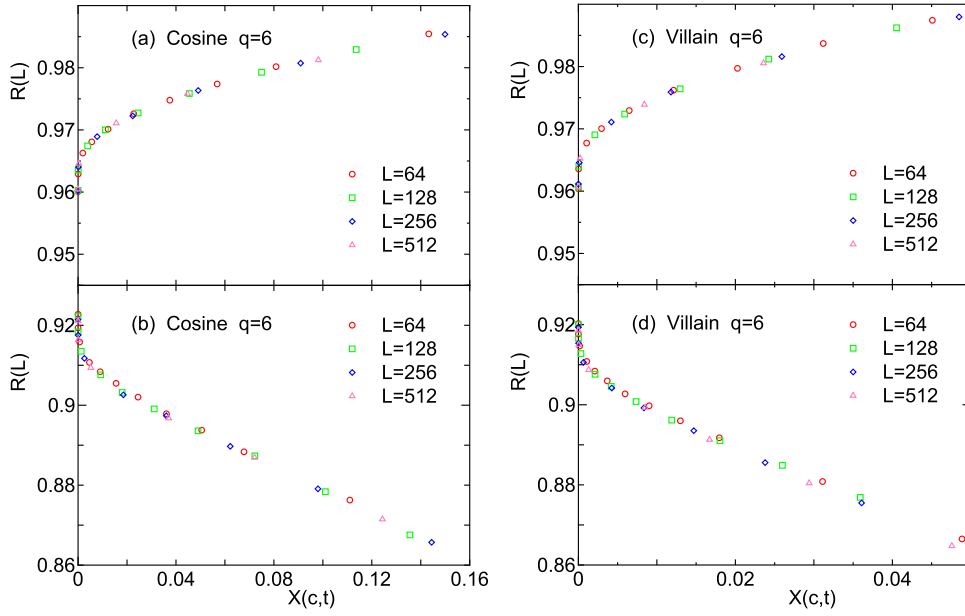


**Figure 5.** The FSS plot of correlation ratio for the estimate of transition temperatures of  $q = 6$  clock model. The scaled variable for the horizontal axis  $X(c, t)$  is defined by equation (13). The estimated values are: (a)  $T_1 = 0.701(5)$  and (b)  $T_2 = 0.898(5)$  for the regular model, and (c)  $T_1 = 0.826(5)$  and (d)  $T_2 = 1.326(5)$  for the Villain model.

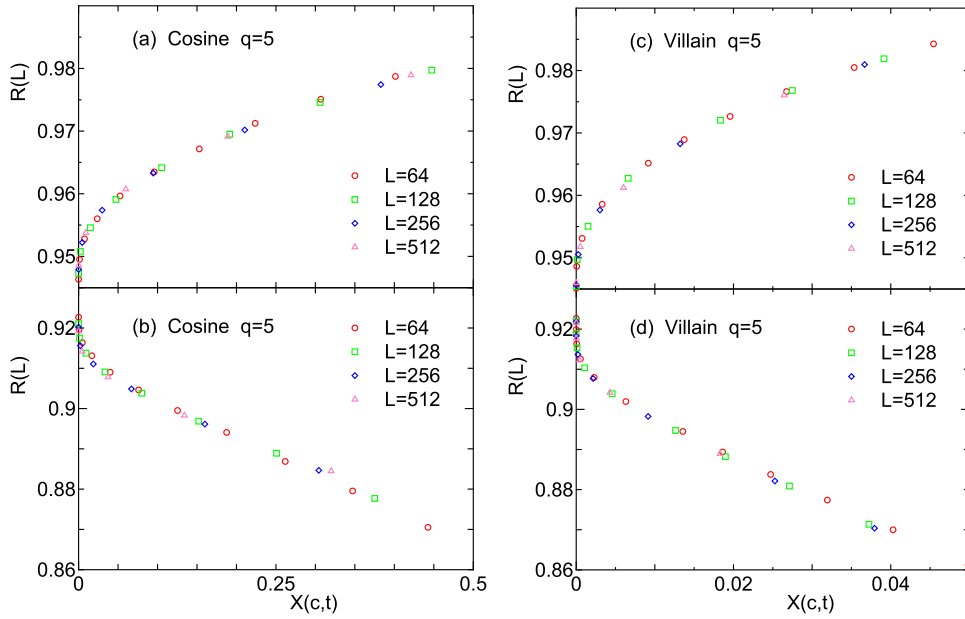


**Figure 6.** The FSS plot of correlation ratio for the estimate of transition temperatures of  $q = 5$  clock model. The scaled variable for the horizontal axis  $X(c, t)$  is defined by equation (13). The estimated values are: (a)  $T_1 = 0.911(5)$  and (b)  $T_2 = 0.940(5)$  for the regular model, and (c)  $T_1 = 1.182(5)$  and (d)  $T_2 = 1.335(5)$  for the Villain model.

**Table 1.** Transition temperatures  $T_1$  and  $T_2$  of  $q$ -state clock models of regular and Villain types for  $q = 5, 6$ . For the Villain types, the duality relation, equation (8), is checked.

$q$	$T_1$	$\eta(T_1)$	$T_2$	$\eta(T_2)$	$T_1 T_2 / (4\pi^2 / q^2)$
6 (regular)	0.701(5)	0.120	0.898(5)	0.236	
5 (regular)	0.911(5)	0.176	0.940(5)	0.234	
6 (Villain)	0.826(5)	0.129	1.326(5)	0.233	1.0002
5 (Villain)	1.182(5)	0.176	1.335(5)	0.235	1.0002

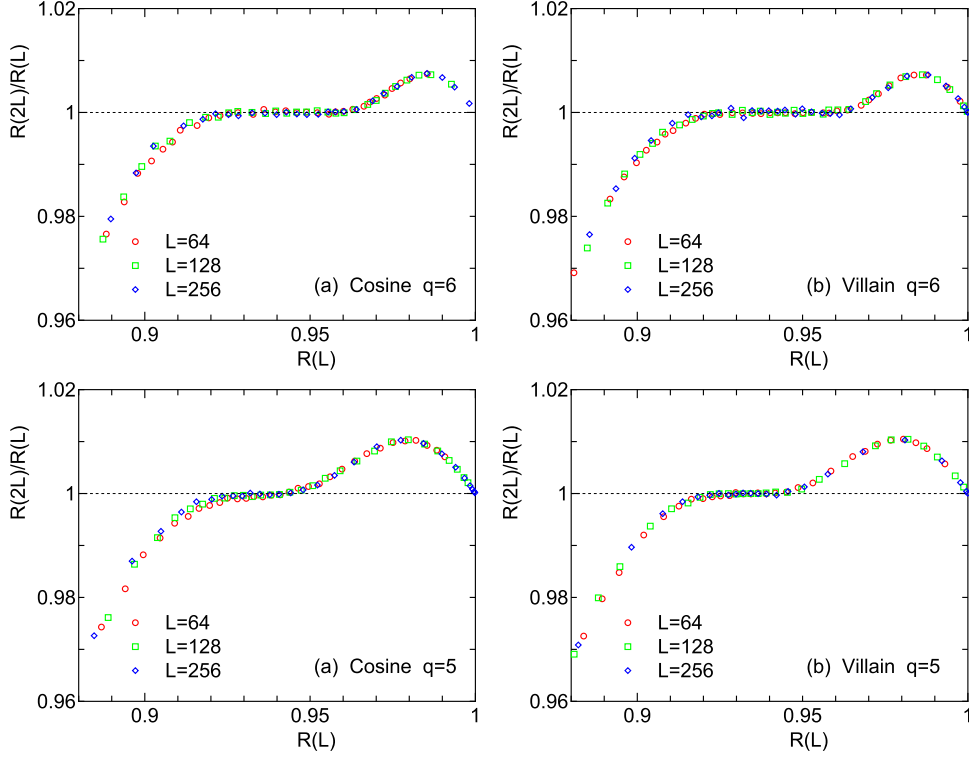


**Figure 7.** FSS plot of  $R(2L)/R(L)$  versus  $R(L)$  of (a) regular and (b) Villain types for  $q = 6$ , and (c) regular and (d) Villain types for  $q = 5$ . The data for the pair of system sizes  $L - 2L$  with  $L = 64, 128, \text{ and } 256$  are shown.

models look the same, but quantitatively two are not identical. This difference becomes larger for  $q = 5$ , because the difference of the local Boltzmann factor becomes larger for high temperatures.

The temperature dependence of decay exponent  $\eta(T)$  is extracted from the data of correlation function. This is done based on equation (4),  $g(L) \sim L^{-\eta(T)}$ , from which we obtain the following scaling form,

$$\frac{g_2(L)}{g_2(2L)} = \frac{L^{-\eta} f(L/\xi)}{(2L)^{-\eta} f(2L/\xi)} = 2^\eta \frac{f(L/\xi)}{f(2L/\xi)} \tag{14}$$

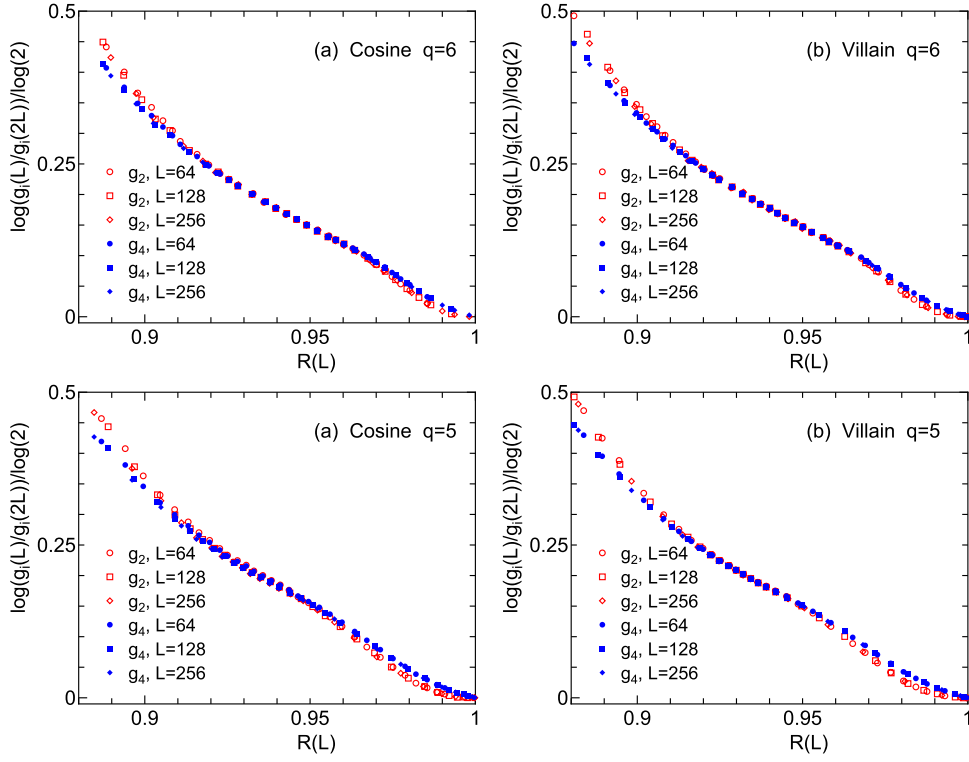


**Figure 8.** FSS plot for the estimate of decay exponent  $\eta$  of (a) regular and (b) Villain types for  $q = 6$ , and (c) regular and (d) Villain types for  $q = 5$ . The value of  $\ln[g_2(L)/g_2(2L)]/\ln 2$  gives  $\eta$  at the temperature of  $R(L)$ .

with  $g_i(L) = g(L/i)$  for the system with linear size  $L$ . By plotting  $\ln[g_2(L)/g_2(2L)]/\ln 2$  with respect to the correlation ratio  $R(L) = g_2(L)/g_4(L)$ , as shown in figure 8, we can obtain the value of  $\eta$  at lower and higher BKT temperatures. The horizontal axis  $R(L)$  can effectively act as temperature axis. Using the estimated values of  $R_1$  and  $R_2$ , we estimate  $\eta(T_1) = 0.120$  and  $\eta(T_2) = 0.236$  for regular model of  $q = 6$ . With this procedure,  $\eta(T_1)$  and  $\eta(T_2)$  are estimated for regular and Villain models with  $q = 6$  and  $q = 5$ . The estimated exponents are tabulated in table 1. We note that the estimated  $\eta(T_2)$ 's are a little bit smaller than the theoretical value of  $1/4$ . At the same time, the estimated  $\eta(T_1)$ 's are a little bit larger than the theoretical value of  $4/q^2$  [11], that is,  $1/9 = 0.1111$  for  $q = 6$  and  $4/25 = 0.16$  for  $q = 5$ . This small systematical deviation is attributed to the logarithmic corrections [5, 41].

#### 4. Summary and discussions

We have investigated 2D  $q$ -state clock models of regular (cosine) and Villain type for  $q = 5, 6$  by using the large-scale Monte Carlo simulations. By calculating the correlation ratio and the size-dependent correlation length for both types for each value of  $q$ , we observed double transitions at each model. The range of temperature in which BKT phase exists is wider for  $q = 6$  than for  $q = 5$ , for both regular and Villain models. This is an indication that for  $q = 5$ , the discreteness starts to play a major role in creating true LRO at lower temperature, although not yet totally rules out the existence of BKT phase.

Verifying the duality relation for the Villain type, and confirming the universal behavior for regular and Villain types, we conclude that the  $q$ -state clock models have double transitions of BKT type for  $q = 5, 6$ . As for the recent controversy, our result coincides with that of Kumano *et al* [20] and that of Chatelain [21]. Although the helicity modulus has been successfully used in the study of the BKT transition of the XY model, a careful treatment should be taken for the discrete clock models. Kumano *et al* [20] pointed out that the helicity modulus defined with respect to an infinitesimal twist is inappropriate when characterizing the BKT transition of the clock models. We briefly comment on the helicity modulus in appendix A.

We also performed the FSS analysis without estimating  $T_{\text{BKT}}$ . Plotting  $R(2L)/R(L)$  as a function of  $R(L)$  in figure 7, we showed the FSS properties without estimating  $T_{\text{BKT}}$ . We also estimated the critical exponents  $\eta$ 's by the plot given in figure 8 to compare with the theoretical values,  $\eta(T_2) = 1/4$  and  $\eta(T_1) = 4/q^2$  [11].

In the case of  $q = 4$ , the clock model becomes equivalent to two sets of Ising model, and exhibits 2nd-order transition. It is instructive to show the present analysis in the case of the 2nd-order transition. We show the data of  $q = 4$  for both regular and Villain models in appendix B.

To summarize, we have shown that  $q$ -state clock models exhibit double BKT transitions for regular and Villain types for  $q > 4$ , although the region of BKT phase is narrow for  $q = 5$  regular clock model, and the corrections to scaling are large for this case. It will be interesting to see the phase diagram of the clock model, that is, the plot of transition temperatures as a function of  $q$ , which is given in appendix C.

## Acknowledgments

The authors wish to thank Toshihiko Takayama for valuable discussions. This work was supported by a Grant-in-Aid for Scientific Research from the Japan Society for the Promotion of Science. TS is grateful to Japan Student Service Organization (JASSO) for its hospitality and to KLN research grant of Hasanuddin University, FY 2018.

## Appendix A. Helicity modulus

The helicity modulus can be expressed as

$$\Upsilon = \langle e \rangle - \frac{L^2}{T} \langle s^2 \rangle \quad (\text{A.1})$$

where

$$e = \frac{1}{L^2} \sum_{\langle ij \rangle_x} \cos(\theta_i - \theta_j), \quad (\text{A.2})$$

$$s = \frac{1}{L^2} \sum_{\langle ij \rangle_x} \sin(\theta_i - \theta_j), \quad (\text{A.3})$$

and the sum is over all links in one direction.

The helicity modulus  $\Upsilon$  is plotted in figure A1 as a function of temperature for the regular model with  $q = 6$  and  $q = 5$ . The universal jump is expected at the point where  $\Upsilon = 2T/\pi$ . The estimate of  $T_2$  by the assumption [42, 43]

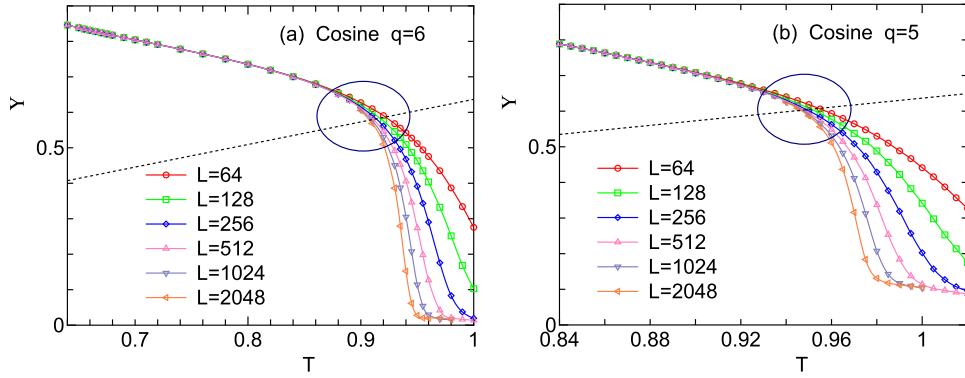


**Figure A1.** The helicity modulus  $\Upsilon$  as a function of temperature for the regular model with (a)  $q = 6$  and (b)  $q = 5$ . The universal jump is expected at the point where  $\Upsilon = 2T/\pi$ .

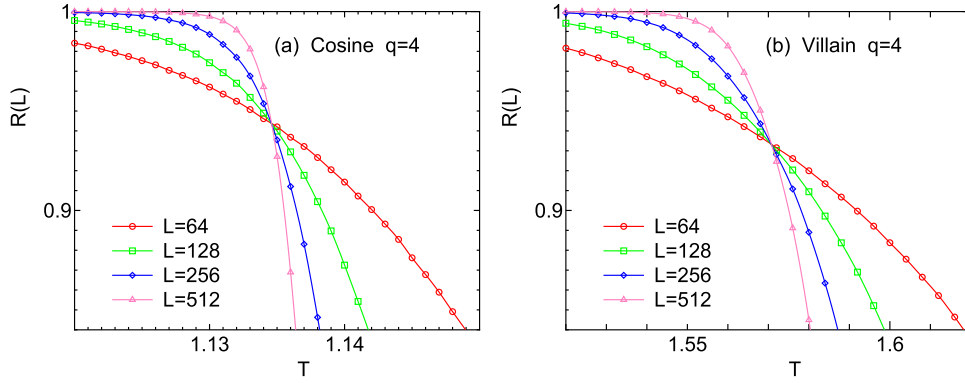


**Figure B1.** Temperature dependence of correlation ratio,  $R(L) = g(L/2)/g(L/4)$ , for (a) regular and (b) Villain types for  $q = 4$ . The crossing of the data with different system sizes gives the 2nd-order transition temperature  $T_c$ .

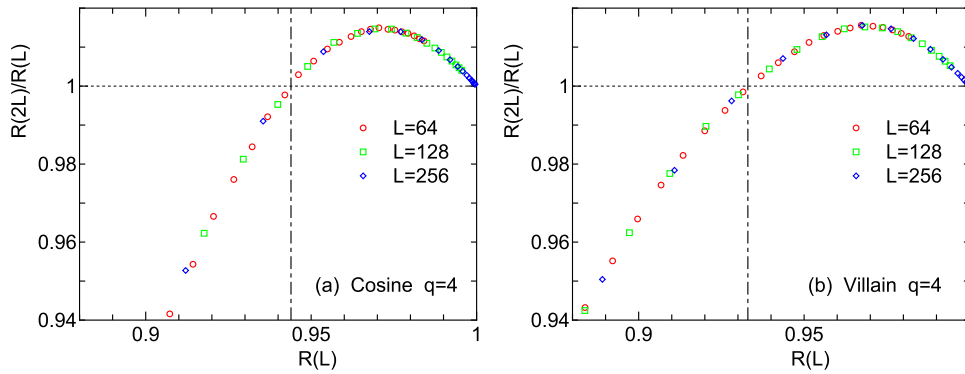


**Figure B2.** FSS plot of  $R(2L)/R(L)$  versus  $R(L)$  of (a) regular and (b) Villain types for  $q = 4$ . The data for the pair of system sizes  $L - 2L$  with  $L = 64, 128,$  and  $256$  are given. The value of  $R_c$  is shown by the vertical dot-dashed line, for convenience.

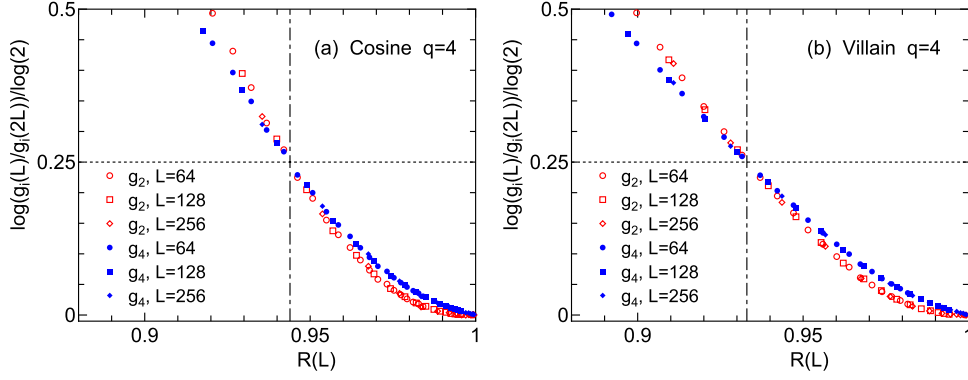


**Figure B3.** FSS plot for the estimate of decay exponent  $\eta$  of (a) regular and (b) Villain types for  $q = 4$ . The value of  $\ln[g_i(L)/g_i(2L)]/\ln 2$  with  $i = 2, 4$  at the critical value of  $R(L)$ ,  $R_c$ , gives the estimate of  $\eta$ . The vertical dot-dashed line shows the value of  $R_c$ .

$$\frac{\pi\Upsilon}{2T} \propto 1 + \frac{1}{2\ln[L/L_0(T)]} \quad (\text{A.4})$$

gives consistent values with the estimates by FSS analysis tabulated in table 1. There are no singularities at  $T_1$ , which means that the helicity modulus is not a good estimator to probe the lower BKT transition.

The authors of [18] claimed that the transition for 5-state clock model is not BKT type as the helicity modulus does not vanish above temperature transition. One proposal to reconcile this discrepancy was presented by Kumano *et al* [20]. They argued that the correct way of calculating helicity modulus for the clock model has to take into account the existing  $Z_q$  discrete symmetry, which is done by a finite, quantized twist rather than the infinitesimal twist [18].

The critical anomaly associated with the higher BKT transition appears near the temperature where  $\Upsilon = 2T/\pi$ ; this region is encircled in figure A1. We note that the tiny correction to the critical value of  $2/\pi$  due to winding field for periodic boundary conditions was calculated by Hasenbusch [44], but the difference is less than 0.02%. From figure A1(b), we see that the helicity modulus remains around 0.1 even for large enough size  $L = 2048$  above  $T_2$ , say at  $T = 0.98$ . The size dependence is small. We also see a remnant of such behavior for  $q = 6$ , which is shown in figure A1(a); the helicity modulus remains 0.02, say at  $T = 0.95$ , for large size  $L = 2048$ . To eliminate this remnant, one needs to modify the form of helicity modulus when probing the BKT phase of clock models as has been described by Kumano *et al* [20].

## Appendix B. Data for $q = 4$

In the case of  $q = 4$ , the clock model becomes equivalent to two sets of Ising model, and exhibits 2nd-order transition. We show the data of  $q = 4$  for both regular and Villain models for convenience. The correlation ratios  $R(L)$  of regular and Villain models for  $q = 4$  are given in figure B1. We observe the crossing of the data at the 2nd-order transition points. For the

**Table C1.** Transition temperatures  $T_1$  and  $T_2$  of  $q$ -state clock models of regular and Villain types for  $q = 4, 5, 6, 8,$  and  $12$ . (a) Present study. (b) [23]. (c) [46]. (d) [36]. For  $q = 4$ , the second-order critical temperatures ( $T_1 = T_2$ ) are exact.

$q$	regular model		Villain model	
	$T_1$	$T_2$	$T_1$	$T_2$
4	1.1346	1.1346	1.5708	1.5708
5	0.911(5) <sup>(a)</sup>	0.940(5) <sup>(a)</sup>	1.182(5) <sup>(a)</sup>	1.335(5) <sup>(a)</sup>
6	0.701(5) <sup>(a)</sup>	0.898(5) <sup>(a)</sup>	0.826(5) <sup>(a)</sup>	1.326(5) <sup>(a)</sup>
6	0.7014(11) <sup>(b)</sup>	0.9008(6) <sup>(b)</sup>	0.8266(18) <sup>(c)</sup>	1.3269(12) <sup>(c)</sup>
8	0.4259(4) <sup>(b)</sup>	0.8936(7) <sup>(b)</sup>	0.4659(6) <sup>(c)</sup>	1.3266(11) <sup>(c)</sup>
12	0.1978(5) <sup>(b)</sup>	0.8937(6) <sup>(b)</sup>	0.2072(3) <sup>(c)</sup>	1.3272(11) <sup>(c)</sup>
$\infty$	—	0.8933(6) <sup>(b)</sup>	—	1.3306 <sup>(d)</sup>

regular model,  $T_c$  is exactly given by  $1/\ln(1 + \sqrt{2}) = 1.1346$ , and for the Villain model,  $T_c$  is given by  $\pi/2 = 1.5708$ . The estimates of  $T_c$  from the crossing of the data reproduce the exact values well. The expression of the critical value  $R_c$  for the regular model can be given in terms of the Jacobi  $\theta$  functions [45], and the exact numerical value becomes  $0.943905 \dots$  [30]. It is to be noted that the estimated critical value  $R_c$  for the Villain model,  $0.933$ , is different from the value of the regular model.

The plot of  $R(2L)/R(L)$  versus  $R(L)$  for  $L = 64, 128,$  and  $256$  is given in figure B2. We observe a very good FSS. The value of  $R(2L)/R(L)$  becomes 1 at a single point,  $R_c$ , which indicates the 2nd-order transition. It differs from the situation of the BKT transition, where the flat region in this plot, the BKT phase, exists. Since the critical value  $R_c$  is different for the regular and the Villain models, we can say that the FSS function for  $R(2L)/R(L)$  versus  $R(L)$  is not universal.

We plot  $\ln[g_i(L)/g_i(2L)]/\ln 2$  with  $i = 2, 4$  in figure B3. We use the (red) open marks for  $g_2$  and the (blue) closed marks for  $g_4$ . We find that the estimate of  $\eta$  from the value at  $R_c$  is consistent with the exact value  $1/4$  for both regular and Villain models. We also note that the data with  $i = 2$  and those with  $i = 4$  cross at the critical value  $R_c$ . It means that we can estimate  $\eta$  from this plot even if we do not know  $T_c$  or  $R_c$ .

### Appendix C. Phase diagram

We tabulate the critical temperatures of regular and Villain types of clock model in table C1. In this table we add some estimates of previous references [23, 36, 46]. We plot the  $1/q^2$ -dependence of  $T_1$  and  $T_2$  of clock models in figure C1. There, the exact results for  $q = 4$  are also given; for the regular model the Ising singularity occurs at  $T_c = [\ln(\sqrt{2} + 1)]^{-1} = 1.1346$ , and for the Villain model that occurs at  $T_c = \pi/2 = 1.5708$ . The transition temperature  $T_1$  becomes smoothly lower with larger  $q$ ; in the lowest order we find that  $T_1 \propto 1/q^2$ , which is consistent with the theoretical prediction [10, 11]. Figure C1 is the phase diagram of the clock models. The arrow indicates the BKT phase. We see a narrow BKT phase for the regular model of  $q = 5$ .

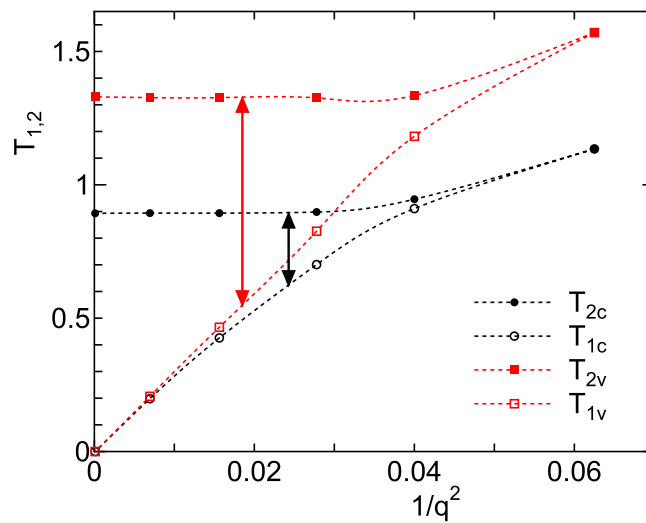


**Figure C1.** Plot of the  $1/q^2$ -dependence of transition temperatures of regular (cosine) and Villain types of clock model. The lower transition temperatures  $T_1$  and the upper transition temperatures  $T_2$  are shown by open and filled marks, respectively. Dotted curves are guided for the eyes. The arrow indicates the BKT phase.

## ORCID iDs

Tasrief Surungan  <https://orcid.org/0000-0003-4943-7628>

Yutaka Okabe  <https://orcid.org/0000-0002-9434-5653>

## References

- [1] Onsager L 1944 *Phys. Rev.* **65** 117
- [2] Mermin N D and Wagner H 1966 *Phys. Rev. Lett.* **17** 1133  
Hohenberg P C 1967 *Phys. Rev.* **158** 383
- [3] Berezinskii V L 1970 *Sov. Phys.—JEPT* **32** 493  
Berezinskii V L 1972 *Sov. Phys.—JEPT* **34** 610
- [4] Kosterlitz J M and Thouless D 1973 *J. Phys. C: Solid State Phys.* **6** 1181
- [5] Kosterlitz J M 1974 *J. Phys. C: Solid State Phys.* **7** 1046
- [6] Resnick D J *et al* 1981 *Phys. Rev. Lett.* **47** 1542
- [7] Marconi V I and Dominguez D 2001 *Phys. Rev. Lett.* **87** 017004
- [8] Vink R L C 2014 *Phys. Rev. E* **90** 062132
- [9] Nahas Y, Prokhorenko S, Kornev I and Bellaiche L 2017 *Phys. Rev. Lett.* **119** 117601
- [10] José J V, Kadanoff L P, Kirkpatrick S and Nelson D R 1977 *Phys. Rev. B* **16** 1217
- [11] Elitzur S, Pearson R B and Shigemitsu J 1979 *Phys. Rev. D* **19** 3698
- [12] Tobochnik J 1982 *Phys. Rev. B* **26** 6201
- [13] Challa M S S and Landau D P 1986 *Phys. Rev. B* **33** 437
- [14] Yamagata A and Ono I 1991 *J. Phys. A: Math. Gen.* **24** 256
- [15] Lapilli C M 2006 *Phys. Rev. Lett.* **96** 140603
- [16] Hwang C-O 2009 *Phys. Rev. E* **80** 042103
- [17] Baek S K, Minnhagen P and Kim B J 2010 *Phys. Rev. E* **81** 063101
- [18] Baek S K and Minnhagen P 2010 *Phys. Rev. E* **82** 031102
- [19] Baek S K, Mäkelä H, Minnhagen P and Kim B J 2013 *Phys. Rev. E* **88** 012125
- [20] Kumano Y, Hukushima K, Tomita Y and Oshikawa M 2013 *Phys. Rev. B* **88** 104427
- [21] Chatelain C 2014 *J. Stat. Mech.* **P11022**

- [22] Villain J 1975 *J. Phys.* **36** 581
- [23] Tomita Y and Okabe Y 2002 *Phys. Rev. B* **65** 184405
- [24] Swendsen R H and Wang J S 1987 *Phys. Rev. Lett.* **58** 86
- [25] Wolff U 1989 *Phys. Rev. Lett.* **62** 361
- [26] Kasteleyn P W and Fortuin C M 1969 *J. Phys. Soc. Japan. Suppl.* **26** 11  
Fortuin C M and Kasteleyn P W 1972 *Physica* **57** 536
- [27] Komura Y and Okabe Y 2012 *Comput. Phys. Commun.* **183** 1155  
Komura Y and Okabe Y 2014 *Comput. Phys. Commun.* **185** 1038
- [28] Nelson D R and Kosterlitz J M 1977 *Phys. Rev. Lett.* **39** 1201
- [29] Minnhagen P and Warren G G 1981 *Phys. Rev. B* **24** 2526
- [30] Tomita Y and Okabe Y 2002 *Phys. Rev. B* **66** 180401
- [31] Surungan T, Okabe Y and Tomita Y 2004 *J. Phys. A: Math. Gen.* **37** 4219  
Surungan T and Okabe Y 2005 *Phys. Rev. B* **71** 188428
- [32] Harada K, Kawashima N and Troyer M 2003 *Phys. Rev. Lett.* **90** 117203
- [33] Kawashima N and Tanabe Y 2007 *Phys. Rev. Lett.* **98** 057202
- [34] Nishimori H 2011 *Elements of Phase Transitions and Critical Phenomena* (Oxford: Oxford University Press)
- [35] Binder K 1981 *Z. Phys. B* **43** 119
- [36] Hasenbusch M and Pinn K 1997 *J. Phys. A* **30** 63  
Hasenbusch M 2008 *J. Stat. Mech.* **P12006**
- [37] Katzgraber H G, Körner M and Young A P 2006 *Phys. Rev. B* **73** 224432
- [38] Komura Y and Okabe Y 2011 *J. Phys. A: Math. Gen.* **44** 015002
- [39] Caracciolo S, Edwards R G, Ferreira S J, Pelissetto A and Sokal A D 1995 *Phys. Rev. Lett.* **74** 2969
- [40] Salas J and Sokal A D 1997 *J. Stat. Phys.* **88** 567
- [41] Janke W 1997 *Phys. Rev. B* **55** 3580
- [42] Weber H and Minnhagen P 1988 *Phys. Rev. B* **37** 5986
- [43] Harada K and Kawashima N 1997 *Phys. Rev. B* **55** 011949
- [44] Hasenbusch M 2005 *J. Phys. A: Math. Gen.* **38** 5869
- [45] Di Francesco P, Saleur H and Suber J-B 1987 *Nucl. Phys. B* **290** 527  
Di Francesco P, Saleur H and Suber J-B 1988 *Europhys. Lett.* **5** 95
- [46] Takayama T 2007 *Master Thesis* Tokyo Metropolitan University